8. O. B. Nielsen, F. de Paoli, K. Overgaard, *J. Physiol.* **536**, 161 (2001).
9. B. S. Launikonis, D. G. Stephenson, *J. Gen. Physiol.* **123**, 231 (2004).
10. G. S. Posterino, G. D. Lamb, D. G. Stephenson, *J. Physiol.* **527**, 131 (2000).
11. G. S. Posterino, T. L. Dutka, G. D. Lamb, *Pflugers Arch.* **442**, 197 (2001).
12. A. L. Hodgkin, P. Horowitz, *J. Physiol.* **148**, 127 (1959).
13. E. M. Balog, R. H. Fitts, *J. Appl. Physiol.* **90**, 228 (2001).
14. B. Hille, *Ion Channels of Excitable Membranes* (Sinauer, Sunderland, MA, ed. 3, 2001).
15. A. F. Dulhunty, *J. Membr. Biol.* **45**, 293 (1979).
16. A. H. Bretag, *Physiol. Rev.* **67**, 618 (1987).
17. J. R. Coonan, G. D. Lamb, *J. Physiol.* **509**, 551 (1998).
18. T. J. Jentsch, V. Stein, F. Weinreich, A. A. Zdebik, *Physiol. Rev.* **82**, 503 (2002).
19. O. F. Hutter, A. E. Warner, *J. Physiol.* **189**, 403 (1967).
20. P. T. Palade, R. L. Barchi, *J. Gen. Physiol.* **69**, 325 (1977).
21. N. Ørtenblad, D. G. Stephenson, *J. Physiol.* **548**, 139 (2003).
22. This research was supported by the Danish Medical Research Council (22-02-0188), University of Aarhus, Australian Research Council, and National Health and Medical Research Council of Australia.

7 June 2004; accepted 27 July 2004

Local Nanomechanical Motion of the Cell Wall of *Saccharomyces cerevisiae*

Andrew E. Pelling, Sadaf Sehati, Edith B. Gralla, Joan S. Valentine, James K. Gimzewski*

We demonstrate that the cell wall of living *Saccharomyces cerevisiae* (baker's yeast) exhibits local temperature-dependent nanomechanical motion at characteristic frequencies. The periodic motions in the range of 0.8 to 1.6 kHz with amplitudes of ~3 nm were measured using the cantilever of an atomic force microscope (AFM). Exposure of the cells to a metabolic inhibitor causes the periodic motion to cease. From the strong frequency dependence on temperature, we derive an activation energy of 58 kJ/mol, which is consistent with the cell's metabolism involving molecular motors such as kinesin, dynein, and myosin. The magnitude of the forces observed (~10 nN) suggests concerted nanomechanical activity is operative in the cell.

Many biological processes taking place inside the living cell rely on the nanomechanical properties of cellular substructures and the cell membrane or wall itself. The atomic force microscope (AFM) (*1*) yields information on the integrity and local nanomechanical properties of mammalian and microbial cellular membranes under normal and stressed metabolic conditions (*2–11*). The sensitivity and ability to apply only minimal forces on a cell makes the AFM a useful nondestructive tool to study cellular nanomechanics. AFM has also been used to measure the natural beating motion in the 0.05 to 0.4 Hz range of cardiomyocytes (heart cells), which is a property related to the cell's physiology (*3*, *12*). In a low-noise environment, the AFM has the sensitivity to measure local nanoscale motion of cells. Here, we have used this capability to discover distinct periodic nanomechanical motion of yeast cells, which we relate to metabolic processes within the cell.

In a typical image of a dense layer of yeast cells air dried onto a mica surface (Fig. 1), yeast

Department of Chemistry and Biochemistry, University of California, Los Angeles, 607 Charles E. Young Drive East, Los Angeles, CA 90095, USA.

*To whom correspondence should be addressed. E-mail: gim@chem.ucla.edu.

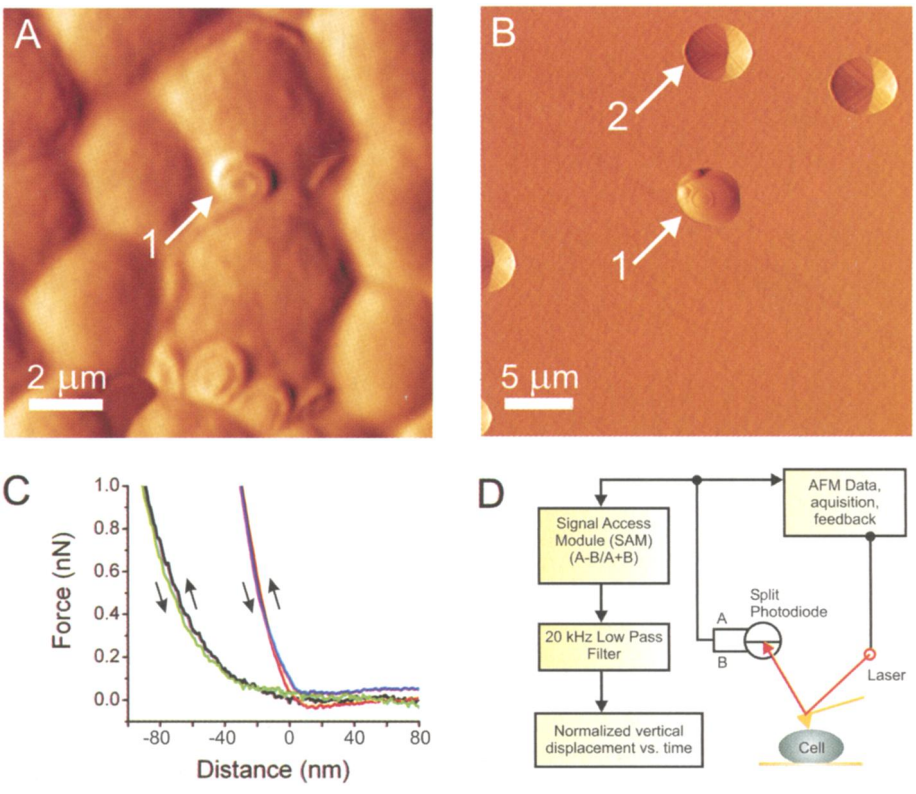

Fig. 1. Typical deflection mode images of yeast cells are shown in (**A** and **B**) [the color scale bar in (A) corresponds to deflections between 0 to 320 nm and 0 to 120 nm in (B)]. A dense layer of yeast cells dried onto mica and imaged in air is shown in (A). Yeast cells are about 5 μm in diameter and often have bud scars on the cell surface (arrow 1). Mechanical trapping is used to study live cells in YPD medium at 30°C. In (B), a typical image of a living yeast cell (arrow 1) trapped in a 5-μm filter pore is shown [empty pores (arrow 2) are easily distinguishable from trapped cells in the image]. Force-distance curves (**C**) can be obtained by monitoring the deflection of the cantilever as it is extended (up arrow) and retracted (down arrow) from the cell in order to measure the local cellular nanomechanical properties. The zero point on the displacement scale represents the point where the AFM tip first comes into contact with the cell. A force-distance curve on the cell body (black line, extension; and green line, retraction) and the bud scar (blue line, extension; and red line, retraction) are shown. Local nanomechanical spring constants (k_{cell}) can be determined from the slope of the linear portion of the curves. Bud scars always display higher k_{cell} because of the increased chitin content of the area (*8*). A schematic of the experimental setup (**D**) outlines the process of measuring the local nanomechanical motion of the cell wall. The AFM cantilever is positioned on top of a living cell, and the scan size is set to 0 nm. The deflection of the cantilever is measured with a photodiode. The signal is acquired with a breakout box (SAM, signal access module), low-pass filtered (20 kHz), and sampled using another computer at 40 kHz.

cells are approximately round and have a diameter of about 2 to 10 μm on average. The disk-shaped protrusion on the cell surface, clearly visible in Fig. 1A, is a bud scar. This structure forms on the cell after the process of division has taken place. Round microbial cells, such as yeast, are quite difficult to immobilize on a surface in liquid so they can be kept alive in order to be studied with the AFM. To circumvent this problem, a technique known as mechanical trapping is used to study single, living round-shaped microbial cells in AFM experiments without the use of chemical immobilizers under physiological conditions in fluid (*8*, *13*, *14*). Cells were first cultured and suspended in yeast extract, peptone, and dextrose (YPD) medium, by using standard techniques (*14*) and were studied at the end of log phase (*15*), which is when the cells are not dividing rapidly and are moving into stationary phase. The suspension was filtered through a polycarbonate membrane, whose ~5-μm pores act as mechanical traps for the cells. The filter was then attached to a petri dish, immediately covered with YPD medium, transferred to the AFM, and left to thermally equilibrate for 1 hour (*14*).

After initial AFM scans of the surface (Fig. 1B), individual cells were selected for force-distance curves to determine the contact force, which was minimized to less than 1 nN. Cantilevers with very low experimentally determined spring constants, k, were used to minimize damage to the cell wall [0.05 ± 0.01 N/m (*16*)]. The local spring constant of the cell wall (k_{cell}) was determined from the slope of the linear portion of the force-distance curve (*17*), which was similar to or slightly larger than that of the cantilever (Fig. 1C). Cell bodies have local k_{cell} of 0.06 ± 0.025 N/m (n = 15). Note that spring constants measured in the same manner on mammalian cells are invariably much lower (~0.002 N/m) (*17*). Yeast cells have a thick cell wall, which accounts for their high local stiffness (*8*). The observed variability in local k_{cell} has been attributed to the heterogeneous chemical makeup of the cell wall and the local nanomechanical properties at the time of measurement (*8*). The cantilever and cell wall can be considered as two springs in series (*14*). Given the cell's local stiffness, we can accurately measure the natural motion of the cell wall. Nanomechanical motion of the cell was observed by recording the cantilever motion (*3*, *7*, *12*) (Fig. 1D), while in contact with the cell, as a function of time in an acoustically isolated environment with a root mean square (rms) noise level of 0.06 nm. We examined nanomechanical motion between 22° and 30°C, using a controllable temperature stage (*14*).

The motion of the cell body of a typical yeast cell recorded at a temperature of 30°C is shown by several examples in Fig. 2. The signal observed is clearly oscillatory with average amplitude of 3.0 ± 0.5 nm (Fig. 2, A to E). The motion was typical for ~70% of the observation times at all temperatures (over 100 experiments were performed over a course of a year, on different individual cells and cell cultures). Occasionally the amplitude would be observed to go as high as 7 nm (Fig. 2F) or to drop as low as 1 nm (Fig. 2G). Fourier transforming the recorded motion revealed a characteristic frequency with a prominent peak at ~1.6 kHz (Fig. 3A). The observed frequencies at any given temperature were similar to within 5% on different cells in one experiment or on different runs with fresh samples of cells.

The results suggest that one of two principal mechanisms is responsible for the observed mechanical oscillations. The motion may be due to an active metabolic process or mechanical resonances and/or Brownian motion. We can differentiate these mechanisms by treating the cells with sodium azide (NaN_3), which is a

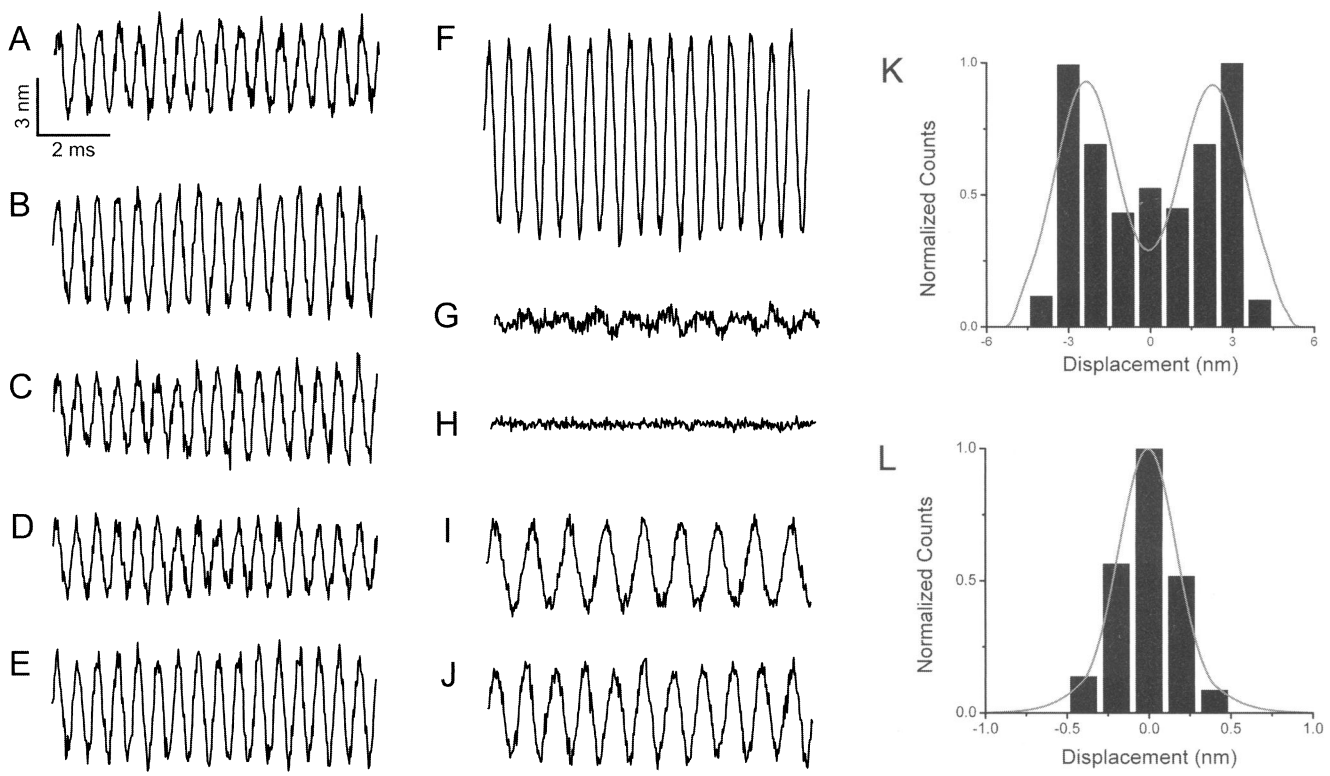

Fig. 2. Typical time traces of the motion of the cell wall of living yeast. All data shown are representative of more than 100 individual experiments carried out on different cells from different cell cultures. The data in (A to G) are from one single cell and data in (H to J) are measurements on different individual cells on different days. In most experimental runs (~70%), the amplitude of the motion was ~3 nm at 30°C (**A** to **D**) but is also consistent at other temperatures as well. Occasionally, amplitudes as large as 7 nm (**F**) and as small as 1 nm (**G**) were observed. In both extremes, the motion is clearly still oscillatory. When cells were maintained at 22°C (**I**) and 26°C (**J**), the amplitudes were similar, but the frequency decreased (see also Fig. 3). Exposure of the cells to sodium azide for 1 hour (*14*) caused the motion to cease (**H**). Living cells displayed a bimodal distribution of amplitudes [**K**, determined from the data in (A)] whereas cells treated with sodium azide always had a Gaussian distribution [**L**, determined from the data in (H)]. Gray lines are Gaussian fits to the data shown in (K and L).

well-known metabolic inhibitor that switches off ATP production in the mitochondria (*18*). Sodium azide is known not to change the mechanical properties of the cell wall, which we verified by measuring the local Young's modulus of the cell wall before and after exposure to the inhibitor (*14*). Likewise, AFM imaging indicated that the cells did not display any significant morphological changes from living cells. The motion observed in azide-treated cells clearly did not display oscillatory behavior and had an average amplitude of 0.4 ± 0.2 nm (Fig. 2H) with a Gaussian distribution of amplitudes whereas living cells always displayed a bimodal distribution (Fig. 2, K and L). Also, no specific frequency components were seen in the Fourier transform (Fig. 3D).

Nanomechanical oscillatory motion was observed to change in a systematic manner, with the frequency increasing significantly with temperature from 0.9 kHz (22°C) to 1.6 kHz (30°C) (Fig. 3); the average amplitude of the motion was similar (Fig. 2, I and J). The strong frequency dependence on temperature and metabolic state indicates that the nanomechanical motion is biologically driven and requires ATP.

An extensive series of control experiments was performed to exclude any contributions of possible artifacts from the AFM itself to the mechanical motion (*14*). No contact resonances between the AFM tip and the surface were observed when the tip was on hard or soft surfaces. Likewise, the mechanical resonance of the AFM cantilever was determined from a Fourier transform of the measured thermal fluctuations of the free cantilever in fluid at 30°C. The cantilevers used had a free resonance of 3.7 ± 0.3 kHz in fluid, far above the frequencies of the observed oscillations. Other resonances we considered were the *x*, *y*, and *z* modes of the piezoelectric tube scanner (2.3 kHz and 4.5 kHz, respectively), which were also out of the range of the frequencies of the cells.

In terms of mechanical resonances, the Young's modulus (*E*) is approximately proportional to the square of the resonant frequency (ω) (*19*). A measurement of the local Young's modulus of the yeast cell wall at all three temperatures also clearly showed that the average stiffness of the wall (0.72 ± 0.06 MPa at 22°C, 0.75 ± 0.04 MPa at 26°C, and 0.75 ± 0.06 MPa at 30°C) does not follow the expected trend for a mechanical resonator ($E \propto \omega^2$). The mechanical properties of the cell wall also did not change significantly after treatment with sodium azide (0.74 ± 0.05 MPa).

The above results clearly show that the changes in frequencies cannot be ascribed to mechanical resonances of the cell or small parasitic resonances in the AFM system. The observed temperature-dependent frequency shifts and disappearance of any oscillatory motion when the cells are exposed to sodium azide provide compelling evidence that the motion has metabolic origins.

This was confirmed from an expected temperature dependence of frequency (ν) that follows a straight line when plotted in an Arrhenius relation, ln[ν] versus 1/*T*. From the slope of the data, we determine an activation energy (E_a) of 58.15 ± 6.57 kJ mol^{-1} (Fig. 4). This value is consistent with the activation energies required to drive molecular motors such as myosin, kinesin and dynein, which occur in the range of 50 to 100 kJ mol^{-1} (*20*, *21*). These motor proteins exhibit dynamic behavior both inside and at the cell wall of yeast (*18*, *22*). Agreement in the value of the activation energies prompted us to compare our measured frequency with known values of linear velocity for motor proteins.

A calculated linear velocity can be determined by multiplying the observed frequencies by the amplitude of oscillation (~3.0 nm). This provides an indication of the operating speeds required for the proteins [2.6 to 4.9 μm s^{-1}, (*14*)]. Operating speeds of 0.2 to 8 μm s^{-1} for the myosins and 0.02 to 7 μm s^{-1} for the microtubule proteins kinesin and dynein (*23*) have been reported, which are comparable with operating speeds estimated from our nanomechanical measurements. Notably, many processes taking place inside the cell that are mediated by these proteins have been reported with operating speeds 1 to 2 orders of magnitude faster than the individual motor proteins (*23*). The force being generated at the cell wall can be determined by multiplying k_{cell} by the average amplitude of 3 nm, which yields a value of 0.2 nN. However, to determine the active force, we increased the contact force

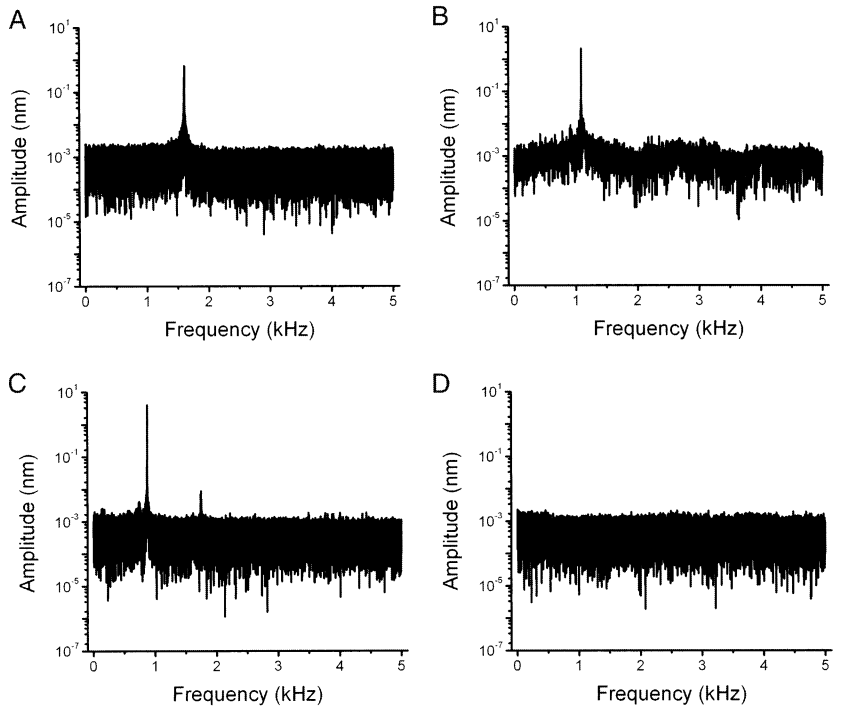

Fig. 3. Fourier transforms of the motion observed in Fig. 2 (note the amplitude is plotted on a logarithmic scale). Each spectrum is from different individual cells at each temperature but is reproducible to within 5% and is representative of many individual measurements. The Fourier transform of the motion at 30°C reveals a prominent peak at 1.634 kHz (**A**). At 26°C at frequency of 1.092 kHz (**B**) is observed and at 22°C a frequency of 0.873 kHz (**C**). Exposure of the cells to sodium azide causes the motion to cease, and no significant frequencies are observed in the Fourier transform (**D**).

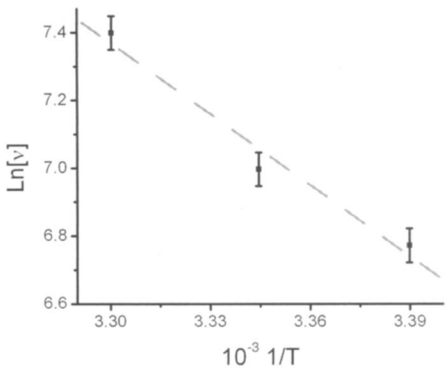

Fig. 4. Arrhenius plots can be constructed for temperature-dependent quantities such as the nanomechanical motion observed in this study. Generally, a temperature-dependent quantity (ν) will follow the relationship $\nu = \nu_0 \exp(-E_a/RT)$, where E_a is the activation energy, *R* is the universal gas constant, *T* is the temperature, and ν_0 the preexponential factor. The equation can be rearranged to take the form of a line where E_a can be determined from the slope: $\ln \nu = \ln \nu_0 - (E_a/RT)$. By plotting the natural logarithm of the frequency (in Hz) (data from Fig. 3, A to C) versus the temperature (1/Kelvin), we determine an E_a of 58.15 ± 6.57 kJ mol^{-1} from the slope of a weighted linear regression fit of the data (dashed line).

from the AFM cantilever on the cell until we noted a change in the amplitude of the motion, which occurred at ~10 nN (*14*). We can exclude that a single motor protein is driving the observed nanomechanical motion, because the forces observed at the cell wall (~10 nN) are far too large in magnitude. This may imply that large-scale forces are generated in yeast cells through the action of many proteins working in a concerted and cooperative manner.

Such cooperativity is known to occur during cell motility and muscle contraction. Spontaneous driven oscillations have been reported in a variety of cells [muscle cells, auditory cells, and structures such as flagella and cilia (*24–26*)], when molecular motors are elastically coupled to their environment by a microtubule or filament. For instance, these oscillations have been experimentally measured between about 1 Hz (muscle fibers) and 300 Hz (flagella) (*27*, *28*). Coupled molecular motors have also been theoretically predicted to be able to achieve frequencies as high as 10 kHz (*24*). These examples of biological processes involving concerted motor protein action lend strong support to our conclusion that a metabolically driven nanomechanical process occurs at the yeast cell wall. This process cannot be observed by traditional cytological methods and occurs in cells in their natural state.

Probing the nanomechanical motion of cell walls is not invasive and does not depend on the use of chemical dyes, fluorescent markers, or quantum dots. The speed of the motion, its response to metabolic inhibitors, and the Arrhenius temperature dependence are completely consistent with active metabolic processes driving the nanomechanical motion. The forces exerted are strongly suggestive of the concerted action of molecular motor proteins. The observed motion may be part of a communication pathway or pumping mechanism by which the yeast cell supplements the passive diffusion of nutrients and/or drives transport of chemicals across the cell wall. The current experiments were performed on yeast cells because they have a stiff cell wall. Extension of this experiment to mammalian cells will require the use of specially fabricated cantilevers with small spring constants comparable to the spring constant of the mammalian cell membrane (~0.002 N/m). Our experiments reveal a new aspect of yeast cell biology—the dynamic nanomechanical activity of the cell wall.

References and Notes

1. G. Binning, C. F. Quate, C. Gerber, *Phys. Rev. Lett.* **56**, 930 (1986).
2. E. A-Hassan *et al.*, *Biophys. J.* **74**, 1564 (1998).
3. J. Domke, W. J. Parak, M. George, H. E. Gaub, M. Radmacher, *Eur. Biophys. J.* **28**, 179 (1999).
4. P. Zhang, A. M. Keleshian, F. Sachs, *Nature* **413**, 428 (2001).
5. C. Rotsch, F. Brate, E. Wisse, M. Radmacher, *Cell Biol. Int.* **21**, 685 (1997).
6. G. T. Charras, M. A. Horton, *Biophys. J.* **82**, 2970 (2002).
7. B. Szabó, D. Selmeczi, Z. Környei, E. Madarász, N. Rozlosnik, *Phys. Rev. E.* **65**, 041910 (2002).
8. A. Touhami, B. Nysten, Y. F. Dufrene, *Langmuir* **19**, 4539 (2003).
9. M. Arnoldi *et al.*, *Phys. Rev. E.* **62**, 1034 (2000).
10. W. R. Bowen, R. W. Lovitt, C. J. Wright, *J. Colloid Interface Sci.* **237**, 54 (2001).
11. M. Gad, A. Itoh, A. Ikai, *Cell Biol. Int.* **21**, 697 (1997).
12. G. N. Maksym *et al.*, *J. Appl. Physiol.* **89**, 1619 (2000).
13. S. Kasas, A. Ikai, *Biophys. J.* **68**, 1678 (1995).
14. Materials and methods are available as supporting material on *Science* Online.
15. M. Johnston, M. Calson, *The Molecular Biology of the Yeast* Saccharomyes: *Gene Expression* (Cold Spring Harbor Laboratory Press, Cold Spring Harbor, NY, 1992).
16. R. Levy, M. Maaloum, *Nanotechnology* **13**, 33 (2003).
17. J. H. Hoh, C. Schoenenberger, *J. Cell Sci.* **107**, 1105 (1994).
18. T. Doyle, D. Botstein, *Proc. Natl. Acad. Sci. U.S.A.* **93**, 3886 (1996).
19. C. M. Harris, *Shock and Vibration Handbook* (McGraw-Hill Book Company, New York, 1988).
20. K. Kawaguchi, S. Ishiwata, *Biochem. Biophys. Res. Comm.* **272**, 895 (2000).
21. K. Kawaguchi, S. Ishiwata, *Cell Motil. Cytoskel.* **49**, 41 (2001).
22. D. Ding, Y. Chikashige, T. Haraguchi, Y. Hiraoka, *J. Cell Sci.* **111**, 701 (1998).
23. J. Howard, *Nature* **389**, 561 (1997).
24. F. Jülicher, *C. R. Acad. Sci. (Paris) Ser. IV* **6**, 849 (2001).
25. A. Vilfan, T. Duke, *Phys. Rev. Lett.* **91**, 114101 (2003).
26. F. Jülicher, J. Prost, *Phys. Rev. Lett.* **78**, 4510 (1997).
27. K. Yasuda, Y. Shindo, S. Ishiwata, *Biophys. J.* **70**, 1823 (1996).
28. S. Kamimura, R. Kamiya, *Nature* **340**, 476 (1989).

29. A.E.P. and J.K.G. gratefully acknowledge C. Ventura (University of Sassari, Italy), M. A. Teitell (University of California, Los Angeles), H. E. Gaub (Ludwig Maximilian University, Munich), D. Kania (Veeco Digital Instruments), and V. Vesna (University of California, Los Angeles) for their insightful discussions and enthusiasm. A.E.P. and J.K.G. thank the Institute for Cell Mimetic Space Exploration, CMISE (a NASA URETI Institute), for partial support. E.B.G., S.S., and J.S.V. thank NIH for support from grant DK46828.

Supporting Online Material

www.sciencemag.org/cgi/content/full/305/5687/1147/DC1
Materials and Methods
Figs. S1 and S2
Tables S1 and S2
References and Notes

29 March 2004; accepted 12 July 2004

Requirement of Rac1 and Rac2 Expression by Mature Dendritic Cells for T Cell Priming

Federica Benvenuti,[1]*† Stephanie Hugues,[1]† Marita Walmsley,[2] Sandra Ruf,[2] Luc Fetler,[3] Michel Popoff,[4] Victor L. J. Tybulewicz,[2] Sebastian Amigorena[1]‡

Upon maturation, dendritic cells (DCs) acquire the unique ability to activate naïve T cells. We used time-lapse video microscopy and two-photon imaging of intact lymph nodes to show that after establishing initial contact between their dendrites and naïve T lymphocytes, mature DCs migrate toward the contacted lymphocytes. Subsequently, the DCs tightly entrap the T cells within a complex net of membrane extensions. The Rho family guanosine triphosphatases Rac1 and Rac2 but not Rho itself control the formation of dendrites in mature DCs, their polarized short-range migration toward T cells, and T cell priming.

In initiating T cell–dependent immune responses, DCs phagocytose antigen in peripheral tissues and migrate to the draining lymph nodes, where they interact with antigen-specific T cells (*1*). To efficiently prime naïve T cells, DCs need to undergo a process of maturation that implies up-regulation of the major histocompatibility complex (MHC) and peptide complexes and the costimulatory molecules at the surface (*2*). Upon maturation, DCs reorganize their actin cytoskeleton (*3*), projecting long and motile membrane extensions, called dendrites, which are likely to facilitate interactions with potentially reactive T cells (*4*, *5*). This type of membrane activity is generally controlled by the actin cytoskeleton, which is in turn regulated by small guanosine triphosphatases (GTPases) of the Rho family (*6*). Although the importance of the actin cytoskeleton and of small Rho family GTPases in T cells during T cell priming has been widely documented (*7*), their role in mature DCs is still unclear (*8–10*).

Interactions between mature DCs and naïve $CD4^+$ T cells during priming were analyzed in vitro with time-lapse video microscopy. DCs projected dendrite-like protrusions around their cell body before T cell contact (Fig. 1A and movie S1). These dendrites, which had an average length of 7 μm, enabled DCs to scan an area up to four times as large as their cell body surface. After an initial dendrite-mediated contact with a T cell, DCs projected numerous mobile membrane extensions and displaced their cell bodies to entangle the lymphocyte. These types of interactions have not been observed with immature DCs, which

[1]Unité INSERM 365, Institut Curie, 26 rue d'Ulm, 75005 Paris, France. [2]Division of Immune Cell Biology, National Institute for Medical Research, Mill Hill, London, NW7 1AA, UK. [3]UMR 168 CNRS/Institut Curie, 11 rue Pierre et Marie Curie, 75005 Paris, France. [4]Institut Pasteur, Unité des Toxines Microbiennes, 75015 Paris, France.

*Present address: International Centre for Genetic Engineering and Biotechnology, Padriciano 99, 34121 Trieste, Italy.
†These authors contributed equally to this work.
‡To whom correspondence should be addressed. E-mail: sebastian.amigorena@curie.fr